International Journal of Nano and Material Sciences, 2017, 6(1): 39-53

Modern Scientific Press

International Journal of Nano and Material Sciences **ISSN: 2166-0182**

Journal homepage: www.ModernScientificPress.com/Journals/ijnanos.aspx *Florida, USA*

Article

Effect of Irradiation on the Structural and Physical Properties of Binary Eutectic Alloys Using Rapidly Solidified from Melt

Adel.S.Waqlan[1, 2]

[1]*Mansoura University, Faculty of Science, Physics Department, Metal Physics Lab, Egypt*

[2] *Physics Department, Faculty of Science and Education, Amran University, Yamen*

* Author to whom correspondence should be addressed; E-Mail: Adel.S.waqlan@gmail.com

Article history: Received 13 June 2017, Revised 19 October 2017, Accepted 24 November 2017, Published 11 December 2017.

Abstract: Microstructure, electrical and mechanical properties of melt-spun Bismuth-Lead, bismuth-tin and bismuth-cadmium eutectic alloys have been investigated using X-ray analysis, the double bridge method and dynamic resonance method. The structure and physical properties of this alloy are affected by the preparation method (rapid solidification technique). X-ray diffraction analysis reveals that melt-spun ribbons with a thickness of 60-120 μm irradiated or unirradiated with the 6MV photon beam, are composed of Pb7Bi3 and Bi phases, and have a single orientation of growth. From the elastic moduli determinations, it is reported that a slight variations of values of Young's modulus with the irradiation effects, because of a very slight disturbance in the structural inhomogeneity. The results show that the irradiated or unirradiated melt-spun ribbons of Bi_{50}-Pb_{50}, Bi_{45}-Sn_{55} and Bi_{50}- Cd_{50}, have a slightly variations in value is observed, in elastic properties and in resistivity measurement.

Keywords: Alloys, Melt-spin technique, Irradiated, Resistivity, Young's modulus and crystallite size.

1. Introduction

Utilizing the chill-block melt-spun technique of rapid quench from the liquid [1], a number alloy systems have been investigated in search of extended terminally solubility ranges or metastable intermediate phases. The existence metastable phase Pb_7Bi_3 was first reported by Claude Borromee-

Copyright © 2017 by Modern Scientific Press Company, Florida, USA

Gautier et al in rapidly solidified lead-bismuth alloy using the splat cooling technique of rapid quench from the liquid [2]. Structure, electrical and mechanical properties of Bi-Pb rapidly solidified eutectic alloy and the effect of the ternary additions have been studied and analyzed [3]. Because bismuth alloys have better properties (very low melting temperatures and low physical strength) for their extensive uses, the aim of the present study is to investigate the electrical and mechanical properties of the rapidly solidified Bi-Pb fusible alloys [4]. Also to study and analyze the effect of ternary and quaternary additions on the structure and some physical properties of Bi-Pb rapidly solidified fusible alloys. Investigated that with the advancement of technology, these is a constant need to develop metallic systems which can be used under a hostile environment of high radiation exposure and can act as the good radiation shield. The material to be used for this purpose, the effect of irradiation on its structure, physical, and mechanical properties should be small. Kuo et al [5] have investigated that the analyses of electron diffraction patterns reveal that the Pb-Bi eutectic nanowire is composed of Pb_7Bi_3 and pure Bi phases, and each of them has the same orientation of growth. Chin-Guo Kuo and Chuen-Guang Chao [6] have confirmed that the X-ray diffraction spectrum showed that the Pb-Bi eutectic alloy Nano scale wires are composed of Pb7Bi3 and Bi phases. The goal of the present study to explore the effects of rapid solidification from melt on the phase's stability of melt-spun ribbons alloys. We first show that the melt-spun ribbons containing two coexisting phases in the Bi-Pb based system utilizing the melt-spinning technique. This is followed by a detailed study on the unirradiated and irradiated by high energy photon irradiation 6MV within these melt-spun ribbon alloys. The Sn-Bi system which is composed of two primary phases at room temperature, bct (body-centered-tetragonal) β-Sn and Rhombohedral Bi and it is a typical single eutectic alloy at 139°C [7]. In the Sn-Pb system, there is also a typical eutectic reaction at 183°C, composed of β-Sn and FCC (face-centered cubic) Pb phases. The Bi-Pb system which the crystalline phases are composed of Rhombohedral Bi, fcc Pb, and hep (hexagonal-close-packed) ε phases, has one eutectic, one paratactic and one eutectoid point at 125.5, 187 and -46°C, respectively. Because of three binary eutectic reactions at relatively low temperatures that constitute the ternary Phase Equilibrium of the Sn-Bi system have been investigated using specific heat measurements [8], and by using calorimetric measurements [9-10]. Kane et al [11] have reported the expansion of primary solid solubility of Bi in Sn. On rapid quenching from the melt below -100 ^{o}C, solubility could be raised from 13.1 at %Bi at the eutectic temperature 139 ^{o}C to 50 at% Bi beyond the eutectic concentration. In 1968 Claude Borromee-Gautier et al [2], observed the existence the metastable phase which is called χ phase and another phase appeared called Y using the splat cooling technique of rapid quenching from the melt. In (1990) [12] Robert Blackwell reported that a low melting point cadmium free fusible lead alloy suitable for custom radiotherapy shielding blocks. Seung Wook Yoon and Hyuck Mo-lee [13] evaluated the thermodynamic parameter of all the

Copyright © 2017 by Modern Scientific Press Company, Florida, USA

stable phase in Bi-Pb binary. They also investigated the thermodynamic properties and phase boundaries of the ternary phase diagram and they found the experimental results agreed with thermal analysis. In (2005)[14] Kuo et al showed that Pb-Bi nanowires have a slightly lower superconductive transition temperature than Pb-Bi eutectic alloy bulk and only about 1% superconductivity volume fraction in magnetic fields both perpendicular and parallel to the plate. Scanning electron microscopy and transmission electron microscopy investigations revealed that nanowire with a diameter of 80nm are composed of Pb_7Bi_3 and Bi phases and have a single orientation of growth. Also, they proved that some properties of Pb-Bi eutectic nanowires using the centrifugal process of melted metal are different from the bulk superconductor.

2. Experimental Procedures

The experimental techniques utilized have been described in details [15-18] and will be explained herein briefly. Three alloys of compositions Bi_{50}-Pb50, Bi_{45}-Sn_{55} and Bi_{50}- Cd_{50}, were prepared in the form of ribbons about 0.4cm wide by about 0.0060-0.0120 cm thickness by ejecting a stream of molten alloy onto a rapidly moving chill surface [19]. The solidification front velocity in the ribbon was estimated to be 30.4m/s. If we assumed that the ribbon becomes completely solid at a distance, d, from the point of impingement of the molten stream, then the solidification rate R is given by:

$$R = \frac{t.v}{d} \quad \ldots\ldots\ldots\ldots\ldots\ldots \quad (1)$$

Where *t* is the ribbon's thickness, v is the surface velocity of the surface wheel. Thus, the solidification rate R is the range 10^{-5}-10^{-4} m/s. Fully solid ribbons can be seen to leave the surface wheel after approximately a tenth of one revolution so that d ≈ 50mm [20]. Due to the small thickness of the samples, the cooling rates can be assumed to be very high. The melt-spun samples under study were irradiated on Elekta medical linear accelerator Shown in Fig.1, by 6 MV photon beam. The samples were put into 30x30x30 cm RW3 slab phantom Shown in Fig.2(a,b), of 10 cm separation at 5 cm depth. The irradiation process was carried out by using two-parallel-opposed field technique which gives a half value of delivered dose from two opposed sides (anterior and posterior) at 100 cm source-to-axial distance (SAD). The total delivered dose was 50 Gy (i.e. 25 Gy from each side) which is given in 2625 MU (monitor unit) by using 25 cm x 25 cm field size. The selection of irradiation type, energy and dose were coming from that dose is considered the most common dose used in the field of radiotherapy.

Techniques used for the subsequent characterization were X-ray diffraction analysis, double bridge method, and dynamic resonance method. X-ray diffraction analysis is carried out with a Shimadzu X-ray diffractometer (Dx-30), using Cu- kα radiation (λ = 0.154056 nm) with a Ni-filter.

Copyright © 2017 by Modern Scientific Press Company, Florida, USA

The measurement of resistivity is carried out by the double bridge method [21]. Elastic moduli melt-spun ribbons were determined by the dynamic resonance method from their mechanical resonance frequencies [22].

Fig. 1. Elekta Linear Accelerator

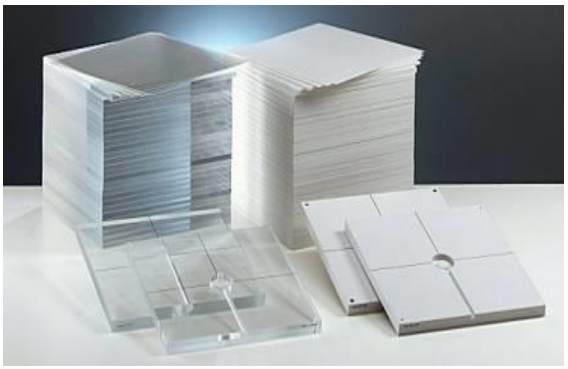

Fig. 2a: PTW RW3 Slab Phantom 30x30x30 cm

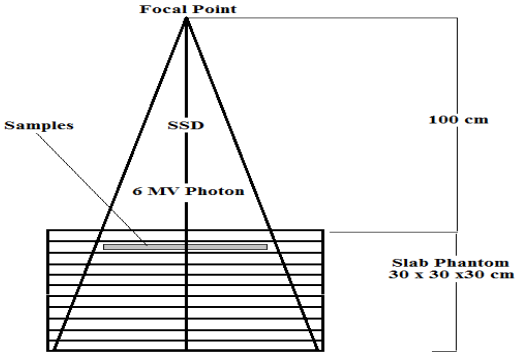

Fig. 2b: Diagram for Samples Irradiation

Copyright © 2017 by Modern Scientific Press Company, Florida, USA

3. Result and Discussions

3.1. Structural Analysis

An analysis of X-ray diffraction lines was made to compare unirradiated and irradiated melt-spun ribbons for binary (Bi_{50}-Pb_{50}, Bi_{45}-Sn_{55}, and Bi_{50}-Cd_{50}) melt-spun ribbons shows that in Fig.3. A very good agreement and confirmed with the results predicted and reported by Claude Borromee-Gautier et al in 1968[2], and the measurements of other authors [3]. They observed the existence of hexagonal close packed phase pb7Bi3 between 30° and 87°. So, the analysis of X-ray diffraction spectrum proves that the alloys metal irradiated or non-irradiated are composed of Pb7Bi3 and Bi phases with a few lines from Sn- and Cd- phases.

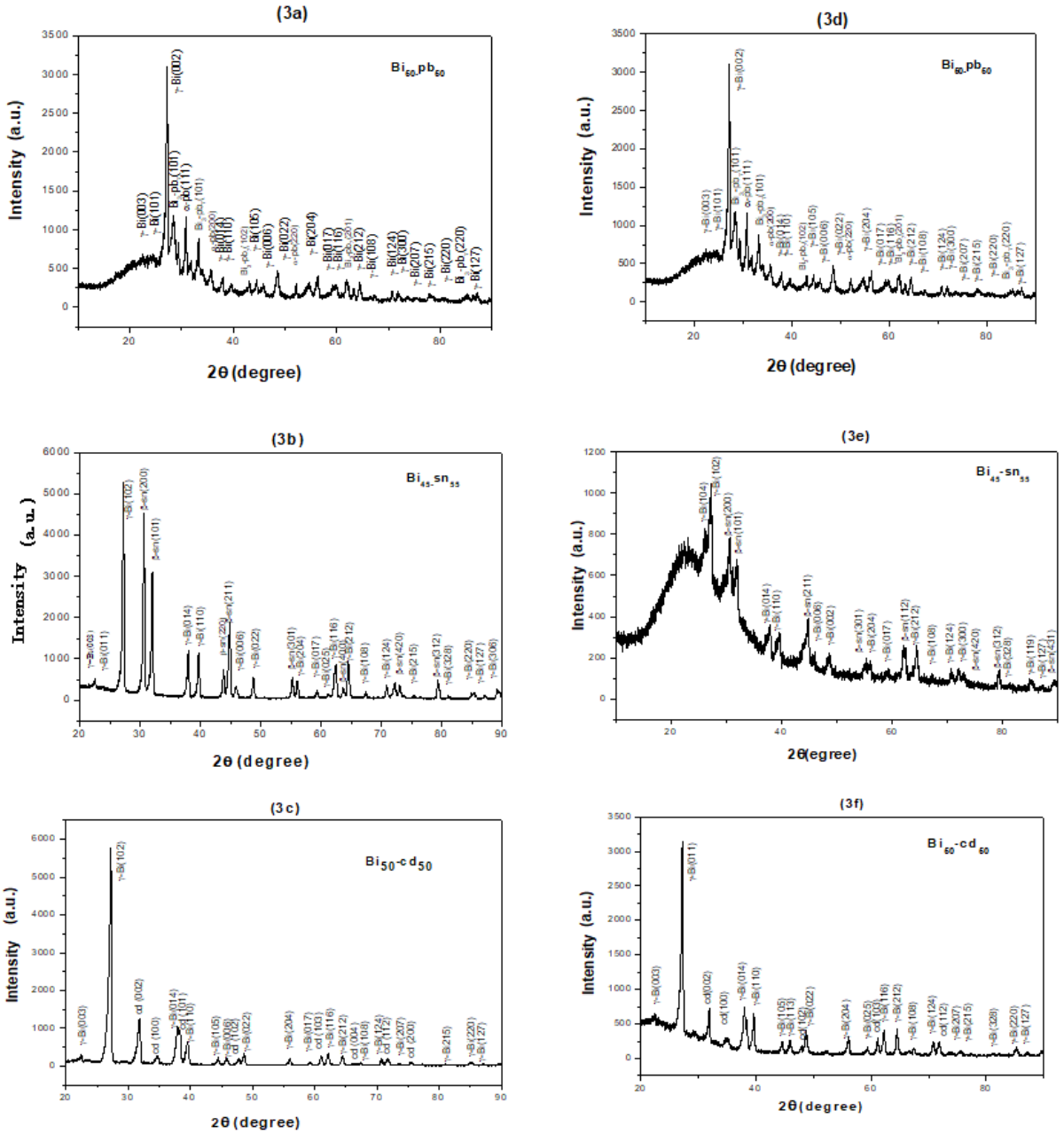

Fig. 3. X-ray diffraction patterns of (a, b, c unirradiated) and (d, e, f irradiated) melt-spun alloys.

Copyright © 2017 by Modern Scientific Press Company, Florida, USA

3.2. Number of Atoms in Unit Cell and Crystallite Size

The next step after identifying the phase and establishing the shape and size of the unit cell is to find the number of atoms in each phase in each melt spun ribbon of the system used in this work. To find this number me use the fact that volume of the unit cell, calculated from the lattice parameters by means of the following equations give the volume V of the unit cell.

Cubic $$V = a^3 \quad \text{..... (2)}$$

Hexagonal $$V = \frac{\sqrt{3}}{2} a^2 c = 0.866 a^2 c \quad \text{..... (3)}$$

Rhombohedra $$V = a^3 \sqrt{1 - 3\cos^2\alpha + 2\cos^3\alpha} \quad \text{..... (4)}$$

So from the following equation

$$\rho = \frac{1.66020 \Sigma A}{V} \quad \text{..... (5)}$$

We have

$$\Sigma A = \frac{\rho V}{1.660202} \quad \text{..... (6)}$$

Where ΣA is the sum of the atomic weights of the atoms in the unit cell, ρ is the density (gm/cm^3), and V is the volume of the unit cell. The number of atoms per cell can calculate from n, where ΣA= n M and M is the molecular weight. When n determined in this way, the number of atoms per cell is always an integer. Within experimental errors, except for some melt-spun ribbons which have defect structure. Table 1, atoms are simply missing from a certain fraction of lattice sites.

Table 1a: Number of atoms per unit cell of Bismuth phases in the following systems

System rapidly solidified from melt	Unirradiated	Irradiated
Bi_{50}-Pb_{50}	1.4	1.3
Bi_{45}-Sn_{55}	1.3	1.4
Bi_{50}-Cd_{50}	1.3	1.2

Table 1b: cell parameters and crystallite size unirradiated and (irradiated).

hexagonal close packed phase Pb_7Bi_3					
composition	a(A^0)	C(A^o)	c/a	Unit cell volume $A^{\circ 3}$	lattice size (A°)
Bi_{50}-Pb_{50}	3.2709 (4.00795)	5.779 (6.0273)	1.7672 (1.50385)	53.544 (83.849)	578.166 (354.979)
Rhombohedral Bi					
composition	a(A^0)	C(A^o)	arho	Unit cell volume $A^{\circ 3}$	lattice size (A°)
Bi_{50}-Pb_{50}	5.170 (4.545)	11.8444 (11.87)	4.96 (4.76)	65.1613 (60.26)	392.4045 (294.214)

Copyright © 2017 by Modern Scientific Press Company, Florida, USA

Table 1c: cell parameters and crystallite size unirradiated and (irradiated)

Tetragonal Sn					
composition	a(A^o)	C(A^o)	c/a	Unit cell volume A$^{\circ 3}$	lattice size (A$^\circ$)
Bi_{45}-Sn_{55}	5.844 (5.8996)	3.1979 (3.1775)	0.58 (0.54)	109.2162 (110.594380)	458.7017 (512.073)

Rhombohedral Bi					
composition	a(A^0)	C (A^0)	a_{rho}	Unit cell volume A$^{\circ 3}$	lattice size (A$^\circ$)
Bi_{45}-Sn_{55}	4.5467 (4.538)	11.8704 (11.904)	4.76 (4.76)	60.25128 (60.33447)	378.764 (5928.868)

Table 1d: cell parameters and crystallite size unirradiated and (irradiated).

Hexagonal Cd					
composition	a(A^0)	C(A^o)	c/a	Unit cell volume A$^{\circ 3}$	lattice size (A$^\circ$)
Bi_{50}-Cd_{50}	2.9789 (2.97697)	5.6255 (5.6158)	1.888 (1.886)	43.23 (43.10)	5.598900 (6.60354)

Rhombohedral Bi					
composition	a(A^0)	C (A^0)	arho	Unit cell volume A$^{\circ 3}$	lattice size (A$^\circ$)
Bi_{50}-Cd_{50}	4.55 (4.402)	11.849 (11.865)	4.755 (4.713)	60.14953 (57.13812)	4.830826 (6.00676)

4. Electrical Properties

In fact, it has observed experimentally that the total resistivity of a metal is the sum of the contributions from thermal vibrations and plastic deformation. This may be presented in a mathematical form as follows:

$$\rho = \rho_t + \rho_i + \rho_d \text{ , } \ldots\ldots\ldots\ldots\ldots\ldots\ldots\ldots\ldots\ldots\ldots\ldots (7)$$

in which ρ_t ,ρ_I ,ρ_d represent the individual thermal, impurity and deformation resistivity contributions respectively. Fig.4 (a, b) shows the electrical resistivity of the melt-spun ribbon alloys used in this part. The electrical resistivity and temperature coefficient of resistivity (T.C.R) values are listed in Table 2. For resistivity measurements, it is found experimentally that Bismuth atoms act as scattering centers [24-25], and increasing the concentrations of bismuth results in an enhancement of resistivity. Bismuth

Copyright © 2017 by Modern Scientific Press Company, Florida, USA

considered as a semimetal has properties somewhere between those of metals and those of semiconductors [23]. Because the overlap in the energy of the bands is usually small 0.03eV in Bi with the Fermi level lying in the region of overlap, the Fermi surface enclose only a small volume in k-space. Thus the number of carriers per unit volume is small compared to typical metals. So in bismuth, it is about $2.7x10^{17}cm^{-3}$. The measured resistivity is summarized in Fig.4 (c, d). The resistivity of all studied before irradiated and same series after irradiated (Bi_{50}-pb_{50}, Bi_{45}-sn_{55}, and Bi_{50}-cd_{50}) alloys. Fig.4 (a, b) shows how the resistivity of the studied samples varies slightly with temperature. The resistivity increased in a stable and useful manner with temperature until the melting point, it meant that electrical conductivity of eutectic solidified alloys decreases with increasing temperature. That is because when the alloys are heated, the thermal vibration of the ions increases, more structural disorder, like vacancies, etc... Are created leading to disorder in periodicity, these factors diffract and scatter the electrons, which reduce the conductivity.

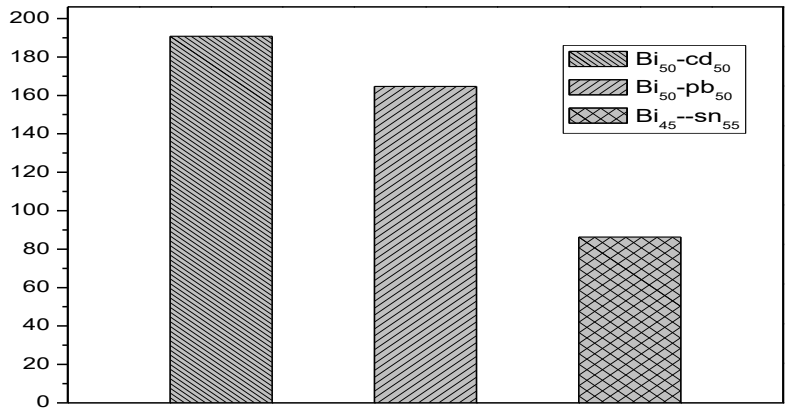

Fig. 4a: Electrical resistivity of Non-irradiated used alloys.

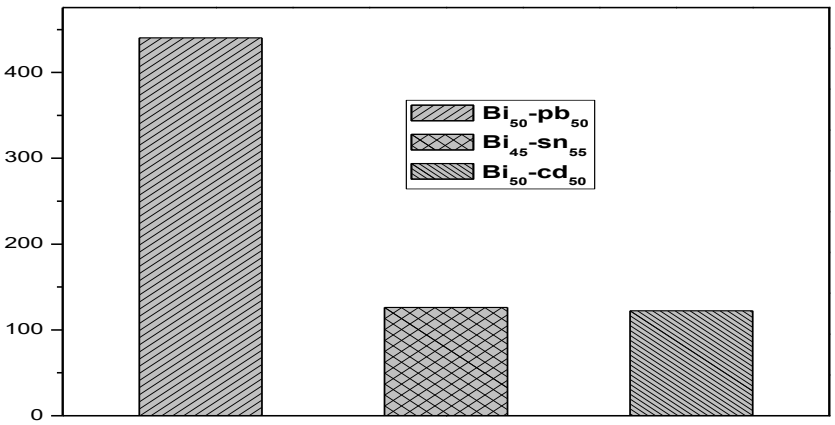

Fig. 4b: Electrical resistivity of irradiated used alloys

Copyright © 2017 by Modern Scientific Press Company, Florida, USA

Table 2: Electrical resistivity and T.C.R of Non-irradiated and (irradiated).

System in Wt.%	Resistivity μΩ.cm	Temperature Coefficient of Resistivity 10^{-3} k^{-1}
Bi_{50}-Pb_{50}	164.7 (440.4)	4.25 (0.0243)
Bi_{45}-Sn_{55}	86.30 (126.1)	2.31 (6.34)
Bi_{50}-Cd_{50}	190.8 (122.2)	2.09 (4.90)

From the above result, it is seen in Table 2, that, the electrical resistivity of Bi_{50}-Cd_{50} of rapidly solidified alloys are much higher than that of Bi_{50}-Pb_{50}, Bi_{45}-Sn_{55}. That is because Cd causes a change in the internal structure, and increases the number of scattering center for conduction electrons. It is seen also in the table (2) that, the electrical resistivity of Bi_{50}-Pb_{50} of rapidly solidified alloys are much higher than the of Bi_{45}-Sn_{55}, Bi_{50}-Cd_{50}.

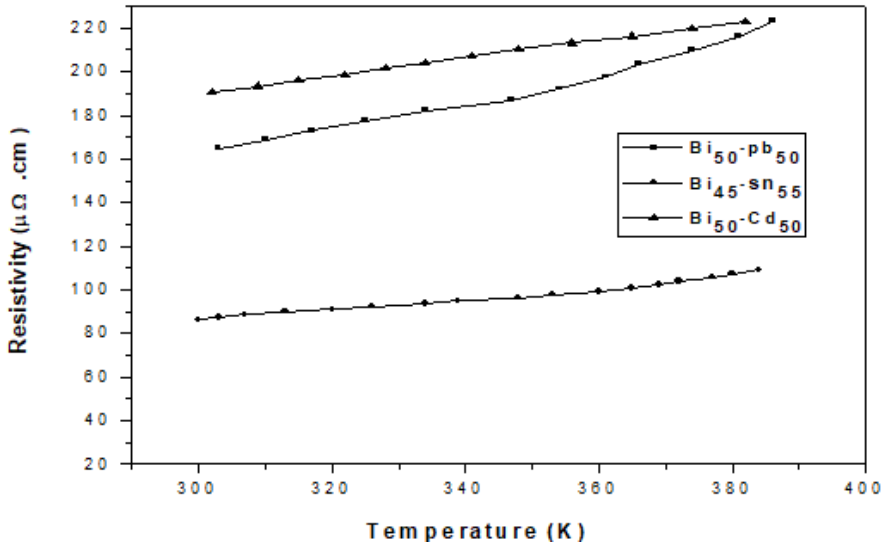

Fig. 4c: Electrical resistivity versus temperature of Non-irradiation used alloys.

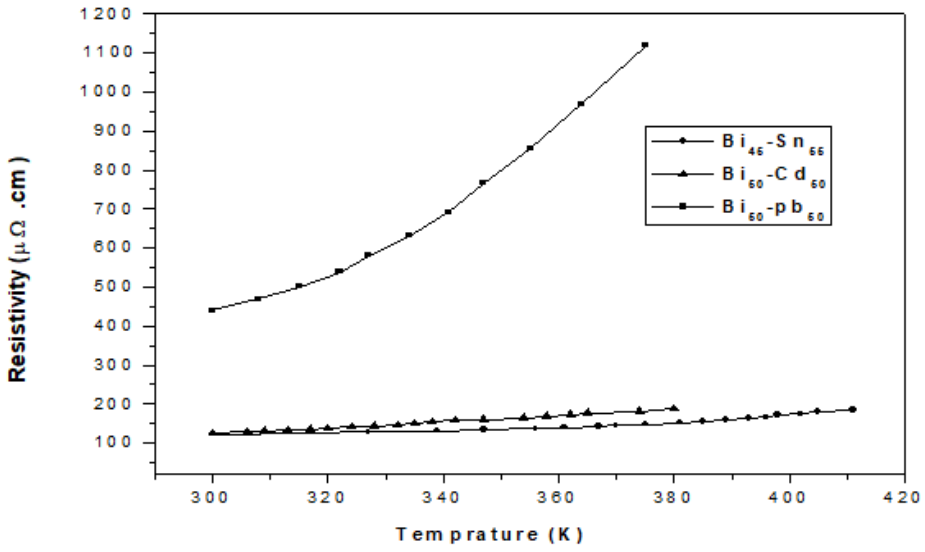

Fig. 4d: Electrical resistivity versus temperature of irradiated used alloys.

Copyright © 2017 by Modern Scientific Press Company, Florida, USA

Conductivity σ is an inverse of electrical resistivity. From an experimental measurement of resistivity ρ of quenched alloys, we can use equation:

$$\sigma = \frac{ne^2\tau_f}{m_e} \quad \ldots\ldots\ldots\ldots\ldots\ldots\ldots\ldots\ldots\ldots\ldots\ldots \quad (8)$$

to estimate the value of the electron density. Table 3, gives a listed of electrical conductivities and other transport parameters such as Fermi energy, Fermi temperature Fermi velocity and Fermi wave vector.

Table 3. Values of Fermi energy, electron concentration, Fermi temperature, Fermi velocities and Fermi wave vector of Non-irradiated and (irradiated) used alloys.

System in wt.%	Conductivity (σ) x10^6 Ω^{-1} m^{-1}	Electron density (n)x10^{28} Electron/m^3	Fermi Energy (E_f) eV	Fermi Wave Vector (k_f)x10^{10} m^{-1}	Fermi Velocity (v_f)x10^6 m/s	Fermi Temperature (T_f)x10^4k
Bi_{50}-Pb_{50}	0.6072 (0.2271)	0.2153 (0.08051)	0.6080 (0.3156)	0.3995 (0.2878)	0.4627 (0.3333)	0.7055 (0.3662)
Bi_{45}-Sn_{55}	1.159 (0.7929)	0.4109 (0.2811)	0.9355 (0.7264)	0.4955 (0.4366)	0.5739 (0.5057)	1.085 (0.8428)
Bi_{50}-Cd_{50}	0.5241 (0.8183)	0.1858 (0.2902)	0.5512 (0.7419)	0.3804 (0.4413)	0.4405 (0.5111)	0.6396 (0.8608)

5. Mechanical Properties

The strength of solid is limited by the atomic bonding force, which is reflected macroscopically by the elastic constant. As a good estimate the theoretical upper bound of the ultimately possible strength is about 0.1of an average elastic stiffness, so that of Young's modulus can serve as a rough criterion for comparison of strengthening the capacity of different materials [26].

Elastic moduli

Most metallic materials of scientific and technological interest are massed together of randomly oriented crystallites. Therefore, the problem of evaluation of the elastic constants (young's modulus, the bulk modulus, the shear modulus and Poisson's ratio) for such polycrystalline metallic materials rapidly solidified from a melt is of great importance in Metal Physics, and in other areas where mechanical properties of aggregates are of interest. Ledbetter, (1977) reported a theoretical basis for the experimental relationship between young's modulus and the shear modulus which has been identified for many years as $G/E = 0.375$. In these study, the value of G/E obtained shows a relative

Copyright © 2017 by Modern Scientific Press Company, Florida, USA

agreement with Ledbetter theoretically values of G/E. Fig.5 (a, **b**) illustrates the elastic modulus of the samples under investigation. The values of elastic moduli may then be computed from the equations:

$$B = \frac{E}{3(1-2v)} \quad \text{and} \quad G = \frac{E}{2(1+v)} \ldots\ldots\ldots\ldots\ldots\ldots\ldots \quad (9)$$

By Knowing the Poisson's Ratio, *v*, Where B is the bulk modulus, G shear modulus which is listed in table 4.

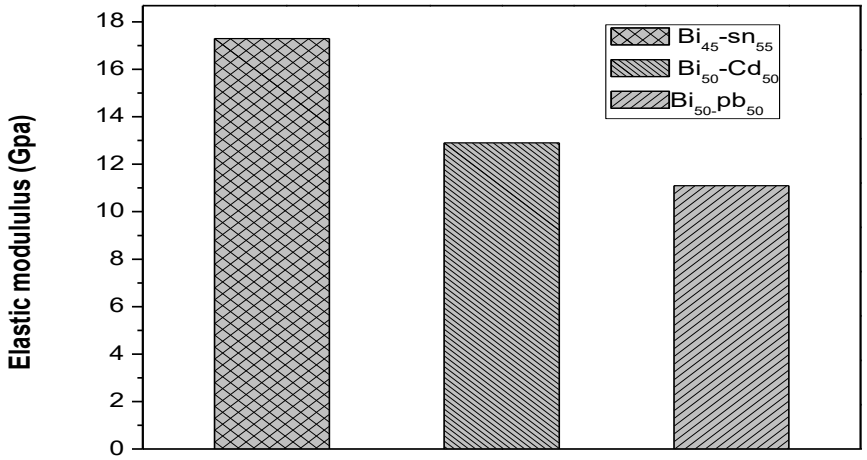

Fig. 5a: Elastic modulus of used non-irradiated alloys.

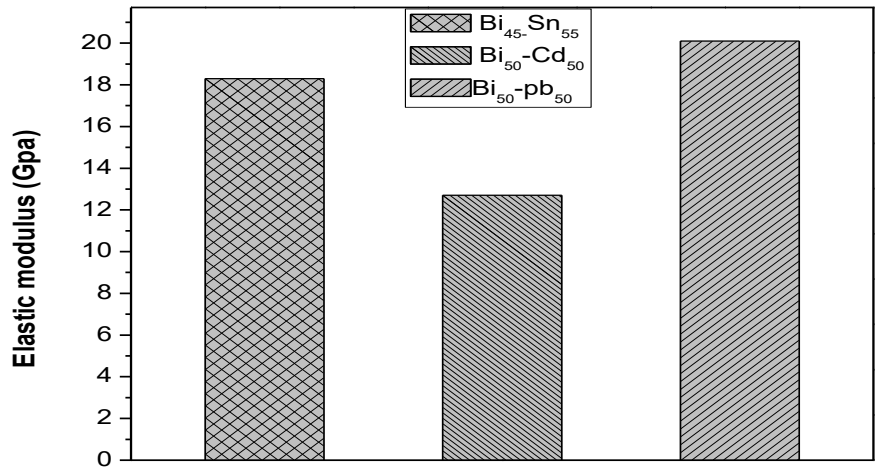

Fig. 5b: Elastic modulus of used irradiated alloys.

Copyright © 2017 by Modern Scientific Press Company, Florida, USA

Table 4a: Elastic modulus of used rapidly solidified non-irradiated and (irradiated) alloys.

System in Wt %	Young's modulus E G Pa	Bulk modulus B G Pa	Shear modulus G G Pa	Poisson's ratio	G/E
Bi_{50}-Pb_{50}	11.1 (20.1)	15.4 (27.9)	4.02 (7.29)	0.38 (0.38)	0.362 (0.362)
Bi_{45}-Sn_{55}	17.3 (18.3)	17 (18)	6.51 (6.89)	0.33 (0.33)	0.376 (0.376)
Bi_{50}-Cd_{50}	18.8 (12.7)	16.9 (11.4)	7.14 (4.82)	0.315 (0.315)	0.379 (0.379)

Internal friction and thermal diffusivity

The name internal friction is usually applied to the broader study of damping from all possible cause. Internal friction measurement is one of the sensitive methods that are suitable for investigating microstructural changes and defect motion, such as atomic diffusion, dislocation activity, and grain boundary sliding. The internal friction Q^{-1} values which calculated from resonance peak shows in Fig.6 (a, b) and given in Table 5.

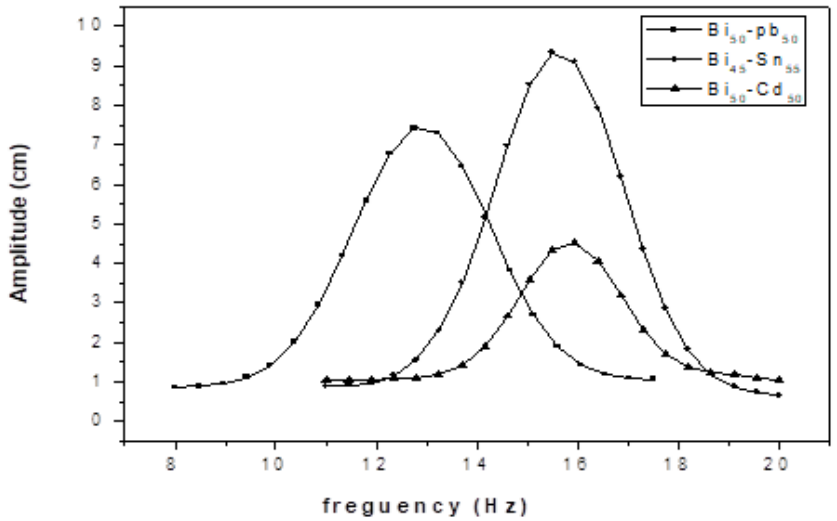

Fig. 6a: Resonance curves of rapidly solidified used non-irradiated alloys.

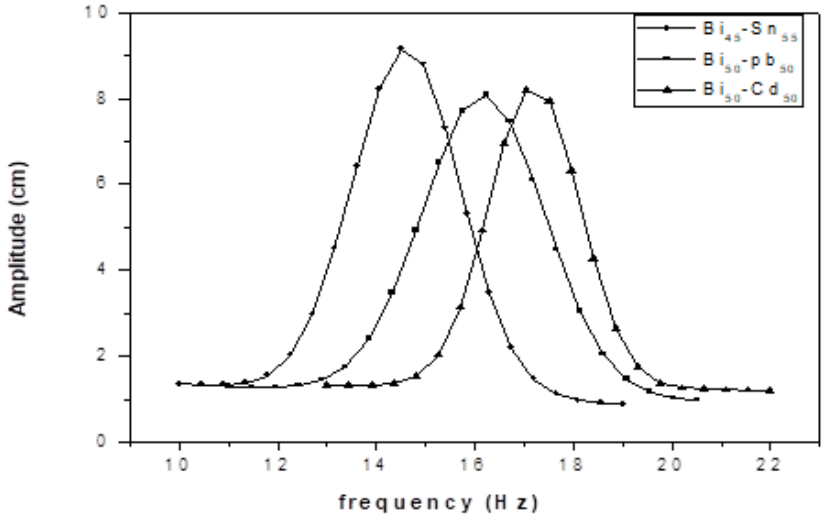

Fig.6.b: Resonance curves of rapidly solidified used irradiated alloys.

Copyright © 2017 by Modern Scientific Press Company, Florida, USA

Table 5. Internal friction of rapidly solidified used non-irradiated alloys.

System in Wt. %	Internal friction Q^{-1} (10^{-3})
Bi_{50}-Pb_{50}	47.2 (42.9)
Bi_{45}-Sn_{55}	42.8 (40.2)
Bi_{50}-Cd_{50}	41.4 (36.1)

6. Thermal Conductivity Measurements

The thermal conductivity change is approximately the same way as was developed for the Electrical Conductivity. There is a definite relationship between the electrical and thermal conductivities of the alloy, although the Wiedemann-Franz ratio does not hold. It is found that the value of the thermal conductivity is 6.15 W/mK. This equation is then K (thermal conductivity) = $5.02\sigma Tx10^{-9}$ +0.03[27]. The calculations values of thermal diffusivity D_{th} using dynamic resonance method of rapidly solidified were measured. The values of thermal conductivity and specific heat may then be computed from the equation described.

$$D_{th} = \frac{k}{c.\rho} \quad \ldots\ldots\ldots\ldots\ldots\ldots\ldots\ldots\ldots\ldots\ldots\ldots \quad (10)$$

Table 6, shows the calculated value of thermal diffusivity, thermal conductivity and specific heat capacity at room temperature (27 ^{o}C).

Table 6: Specific heat, thermal diffusivity and thermal conductivity of rapidly solidified used non-irradiated and (irradiated) alloys.

System in Wt.%	Conductivity (σ) x10^6 Ω^{-1} m^{-1}	Density g/cm^3	Thermal Diffusivity D_{th} 10^{-8} m^2/sec	Thermal Conductivity (k) Watt $m^{-1}k^{-1}$	Specific heat Capacity (c) J/kg.k
Bi_{50}-Pb_{50}	0.6072 (0.2271)	7.496 (7.496)	5.23 (7.142)	4.451 (1.676)	1.745 (3.361)
Bi_{45}-Sn_{55}	1.159 (0.7929)	5.716 (5.716)	4.6 (4.78)	8.551 (5.851)	1.134 (1.460)
Bi_{50}-Cd_{50}	0.5241 (0.8183)	7.380 (7.380)	5.65 (7.76)	3.868 (6.039)	1.925 (1.430)

The present part investigated the structure and properties of Bi_{50}-Pb_{50}, Bi_{45}-Sn_{55}, Bi_{50}-Cd_{50} rapidly solidified from a melt. Based on observations described, the following conclusions may be formulated:

7. Conclusion

Copyright © 2017 by Modern Scientific Press Company, Florida, USA

From analyses of X-ray diffraction patterns reveal that the Pb_{50} -B_{i50} metal irradiated or unirradiated rapidly solidified from the melt is composed of Pb_7Bi_3 and Bi-phases, each of them has the same orientation of growth. The electrical resistivity of rapidly solidified Bi_{50}-Pb_{50}, Bi_{45}-Sn_{55} eutectic alloys at 300K after irradiated are much higher than Bi_{50}-pb_{50}, Bi_{45}-Sn_{55}, of the non- irradiated, while in the case Bi_{50}-Cd_{50}, or the electrical resistivity non-irradiated is much higher than that of after irradiated. From the elastic moduli determinations, it is reported that a slight variations of values of Young's modulus with the irradiation effects, because of a very slight disturbance in the structural inhomogeneity. Internal friction of melt-spun metal irradiated is very smaller than that of unirradiated. It is suggested that this is caused by pores.

References

[1] Mustafa Kamal and Usama S. Mohammad, a Review: Chill Melt Spin Technique, *Theories & Applications Bentham*, 2012, PP.42-69.

[2] Claude Borromee- Gautier, Bill C. Giessen, and Nicholas J. Grant, *the Journal of Chemical Physics*, 1968, 48(5): 1905-1911.

[3] Eman Abd El-Wahab, M. Sc. Thesis, *Structure, Thermal, Electrical and Mechanical properties of Bi-Pb based eutectic alloys rapidly quenched from the molten state*, Faculty of Science, Mansoura University, 2003.

[4] A. Bakr and E. Bediwi, Physical properties of melt-spun Bismuth-Lead based fusible alloys, *Radiation Effects and Defects in Solids*, 2004, 159: 75-83.

[5] C. G. KUO, Y.Y. HSU, M.K. WU, C. G. Chao, *Appl. Phys. An, 2005*, 80: 1501-1504.

[6] Chin. GUO KUO and Chuen-Gang Chao, Int. J. Adv. MANUF TECHNOL, 2007, 32, 5: 468-472.

[7] T. B. Massalaki, *Binary Alloy Phase Diagrams*, 2nd ed., ASM, Materials Park, USA.1991.

[8] H. Ohtani and K. Ishida, A thermodynamic study of the phase equilibria in the Bi-Sn-Sb System, *J. Electro.Mater.*1994, 23:747- 756.

[9] G. Ghosh, M. Loomans, M. E. Fine, An investigation of phase equilibria of the Bi-Sb-Sn system, *J. Electron.Mater*.1994, 23:619- 624.

[10] U. R. Kattan et and W. J. Boettinger, On the Sn-Bi-Ag ternary phase diagram, *J. Electro. Mater.*1994, 23: 603-610.

[11] R. H. Kane, B.C. Giessen, and N.J. Grant, *Acta Met.*, 1996, 14: 605.

[12] Blackwell, C. R; Amundson, K. D. Amundson, *Material Dosimetry*, 1990, 15: 127-129.

[13] Seung Wook Yoon and Hyuck Mo Lee, *Calphad*. 1998, 22(2):167-178.

[14] C. G. KUO, Y.Y. HSU, M.K. WU, C. G. Chao, *Appl. Phys. A*, 2005, 80: 1501-1504.

Copyright © 2017 by Modern Scientific Press Company, Florida, USA

[15] Mustafa Kamal, A. B. El-Bediwi, A. R. lashin, A. H. El-Zarka, *Materials Science and Engineering A*, 2011, 530: 327-332.

[16] Mustafa Kamal, A. B. El-Bediwi, and Tarek. El-Ashram, *Journal of Materials Science: Materials in Electronics*, 2004, 15: 211-217.

[17] Mustafa Kamal and Abu-Bakr El-Bediwi, *Radiation Effects and Defects in Solids*, 2004, 159: 651-657.

[18] Mustafa Kamal and El-Said Gouda, *Materials and Manufacturing Processes*, 2006, 21: 736-740.

[19] M. Kamal, J.C. Pier, R. Jouty, *Mëmoires et Etudes Scientifiques Revue de Mëtallurgie-Mars* (1983): 143-148.

[20] R. Cheese, B. Cantor, *Mater. Sci. Eng.* 1980, 45: 83-93.

[21] Y. A. Geller and A. G. Rakhshtadt, *Science of Materials*, Mir Publishers, Moscow, 1977. P138.

[22] E. Schreiber, O. L, Anderson and N. Soga, *Elastic Constants and their Measurement*, Mc Grew-Hill Companies, Inc, New York, 1973, P.82.

[23] M. Kamal and A. B. El-Bediwi, Structure, mechanical metallurgy and electrical transport properties of rapidly solidified Pb50Sn50-xBix alloys, *J. Materials Science Materials in Electronics*, 2000, 11: 519-523.

[24] B.S. Berry and W.C. Pritchett, *J. Appl. Phys.*, 1973, 44: 3122.

[25] C.A. Kukkonen and P. F. Maldague, The electrical resistivity of bismuth: electron-hole scattering, *J. Phys. F: Metal Phys.* 1976, 6(11): 301-302.

[26] K. Anagnostopoulos and J.E. Aubrey, The electrical resistivity of bismuth: intervalley scattering, *J. Phys. F: Metal Phys.* 1976, 6(6): 181-184.

[27] Mustafa Kamal and Abu-Bakr El-Bediwi, *Radiation Effects and Defects in Solids*, 2004, 159: 651-657.

Copyright © 2017 by Modern Scientific Press Company, Florida, USA